Anal. Chem. **2005,** *77,* 2235−2242

Comparison of Photophysical and Colloidal Properties of Biocompatible Semiconductor Nanocrystals Using Fluorescence Correlation Spectroscopy

Sören Doose,*,†,‡ James M. Tsay,† Fabien Pinaud,† and Shimon Weiss*,†,§

Department of Chemistry and Biochemistry and Department of Physiology, University of California at Los Angeles, Los Angeles, California 90095

A number of different surface chemistries have been developed in recent years to render semiconductor nanocrystals (NCs) stable in water and biocompatible. However, most of these surface modifications affect NCs' photophysical properties, calling for a method to simultaneously monitor colloidal and fluorescence properties. Fluorescence correlation spectroscopy (FCS) combined with ensemble spectroscopic methods and Monte Carlo simulations were used to interpret and derive photophysical as well as colloidal properties of four different NC surface treatments. Using a novel FCS scheme with alternating laser excitation at two different intensities, we first ruled out influences from optical gradient forces (optical trapping). We then compared concentration of emitting particles, brightness per particle, saturation intensity, blinking (intermittency), hydrodynamic radius, and propensity for aggregation of the different bioconjugated NCs. This approach was successfully applied during the development and optimization of peptide-coated NCs.

The widespread use of fluorescence techniques in biological research has triggered the development of ever more advanced fluorescent labels. Colloidal semiconductor nanocrystals (NCs) are nanometer-scale inorganic clusters useful for fluorescence labeling in multicolor biological imaging and detection.[1−4] Colloidal NCs consist of an inorganic core (for example, CdSe), an inorganic shell (for example, ZnS), and an organic coating layer that determines their colloidal properties and biocompatibility. For biological applications, NCs must be water-stable. Although synthetic methods exist to grow such particles in water, highest quality NCs are synthesized in nonpolar solvents with hydrophobic coatings such as trioctyl phosphine oxide (TOPO). To render these NCs biologically useful, several surface chemistries that replace the hydrophobic surfactants with hydrophilic coatings have been developed.[5−7] In addition, these surface-modified NCs must be nontoxic to the cell, allow conjugation chemistries for attaching recognition molecules to their surface, and display specific targeting, chemical stability, and photostability. The requirements for their application in single-molecule biological studies can be even more stringent (i) on colloidal properties—fluorescent NCs must display narrow size distribution and smallest possible size (to minimize steric hindrance)—and (ii) on photophysical properties—high quantum yield (QY), reduced blinking,[8,9] and large saturation intensity (to maximize signal-to-noise ratios).

Since NC surface modification chemistries strongly affect their colloidal and photophysical properties, methods are required to monitor all properties each time a chemical modification is made. Currently, photophysical characterization is mostly done using UV/visible absorption and fluorescence spectrophotometry. Colloidal properties, such as particle size, size distribution, and aggregation, are monitored by liquid chromatography, electrophoresis, light scattering, transmission electron microscopy (TEM), and atomic force microscopy (AFM). Excluding the last two (nonoptical techniques), none of these methods provides single-molecule sensitivity. Whereas ensemble techniques are widely used to determine emission and absorption spectra and fluorescence QYs, information on heterogeneous properties, such as blinking (dynamic heterogeneities) and on NC subpopulations of various brightness (sample heterogeneities), cannot be provided without single-molecule techniques.

A number of groups have investigated individual surface-immobilized NCs using CCD imaging and scanning-stage confocal microscopy. Nirmal et al.[8] first detected blinking (intermittency) in the emission of single NCs. This blinking behavior was later determined to follow power law statistics, with on/off time

* Corresponding authors. E-mail: sdoose@chem.ucla.edu; sweiss@chem.ucla.edu. Fax: 310.267.4672.

† Department of Chemistry and Biochemistry.

‡ Current address: Applied Laserphysics & Laserspectroscopy, University of Bielefeld, 33615 Bielefeld, Germany.

§ Department of Physiology.

(1) Bruchez, M., Jr.; Moronne, M.; Gin, P.; Weiss, S.; Alivisato, A. P. *Science* **1998**, *281*, 2013−2016.

(2) Chan, W. C.; Nie, S. *Science* **1998**, *281*, 2016−2018.

(3) Michalet, X.; Pinaud, F.; Lacoste, T. D.; Dahan, M.; Bruchez, M. P.; Alivisato, A. P.; Weiss, S. *Single Mol.* **2001**, *2*, 261−276.

(4) Alivisatos, P. *Nat. Biotechnol.* **2004**, *22*, 47−52.

(5) Wu, X.; Liu, H.; Liu, J.; Haley, K. N.; Treadway, J. A.; Larson, J. P.; Ge, N.; Peale, F.; Bruchez, M. P. *Nat. Biotechnol.* **2003**, *21*, 41−46.

(6) Dubertret, B.; Skourides, P.; Norris, D. J.; Noireaux, V.; Brivanlou, A. H.; Libchaber, A. *Science* **2002**, *298*, 1759−1762.

(7) Pinaud, F.; King, D.; Moore, H. P.; Weiss, S. *J. Am. Chem. Soc.* **2004**, *126*, 6115−6123.

(8) Nirmal, M.; Dabbousi, B. O.; Bawendi, M. G.; Macklin, J. J.; Trautman, J. K.; Harris, T. D.; Brus, L. E. *Nature* **1996**, *383*, 802−804.

(9) Hohng, S.; Ha, T. *J. Am. Chem. Soc.* **2004**, *126*, 1324−1325.

10.1021/ac050035n CCC: $30.25
Published on Web 03/04/2005

distributions being dependent, respectively independent, on both excitation power and temperature.[10,11] The most important consequence of power law statistics is that the average on/off time depends on the experimental observation (integration) time thus making blinking appear on any experimental time scale. Recent work reported near-complete suppression of blinking by varying the buffer conditions.[9] The report supports the interpretation that blinking is caused by surface defects, which can be altered by surface chemistries and buffer conditions. By combining AFM and confocal microscopy, Ebenstein et al.[12] identified the presence of a dark subpopulation of NCs in a sample. Several groups reported ensemble QY changes upon sample illumination (photoinduced activation).[13−15] In light of Ebenstein's results, QY changes could in fact be attributed to brightness heterogeneity with light-induced on/off switching of individual NCs (as opposed to homogeneous changes of QYs). We recently demonstrated this switching mechanism for surface-immobilized TOP/TOPO CdSe/ZnS NCs.[14] Lifetime measurements on single NCs revealed nonexponential fluorescence decays, unlike monoexponential decays for conventional organic dyes.[16,17] These nonexponential decays also suggest static and dynamic heterogeneities in NCs' optical properties. For all these reasons, single-molecule screening methods would be helpful for the optimization of NC surface chemistries.

However, confocal studies of immobilized NCs are slow, low throughput, and inevitably influenced by NC surface immobilization. Comparatively, fluorescence correlation spectroscopy (FCS), performed on diffusing NCs using confocal microscopy, has single-molecule sensitivity and is compatible with high-throughput analysis.[18,19] FCS provides information on mechanisms that generate fluorescence intensity fluctuations by analyzing the correlation function, e.g., diffusion of fluorophores through the observation volume or blinking. Even though the recorded FCS curve is a measurement on a small ensemble of molecules (about nM concentrations), it can provide evidence for *distributions* of characteristic time constants and sample heterogeneities.

FCS has been employed over the past decade in a wide range of biochemical assays.[20−23] It has been applied to monitor conformational fluctuations of biopolymers, detect binding events between macromolecules and their ligands, investigate photophysical properties of organic dyes and fluorescent proteins, or look at diffusion properties of labeled macromolecules in vitro and in vivo. Larson et al.[24] have investigated the potential of NCs as probes in 2-photon (2P) microscopy using 2P-FCS.

FCS has been successfully used to measure particle concentrations, diffusion times (the time required for a molecule to diffuse through the laser focus), and fast photophysical kinetics for various organic fluorophores. Using FCS to characterize NCs, however, is complicated by the effects of overlapping time scales for blinking and diffusion times and the influence of saturation.[25] Optical trapping has also been claimed to alter FCS results.[26−28]

Here we use a combination of ensemble spectroscopies, FCS, and simulations to characterize the photophysical and colloidal properties of different water-stable NCs. We investigate the influence of power law distributed blinking on FCS measurements using simulated trajectories of blinking NCs. With the help of an alternating-laser-excitation scheme (ALEX), we perform simultaneous FCS at two excitation powers (ALEX-FCS), proving that no noticeable optical trapping, photobleaching, or photoinduced activation takes place on time scales comparable to the diffusion time. We further investigate and compare brightness per particle, saturation intensity, blinking, and hydrodynamic radii for different NCs and demonstrate that variations in the FCS amplitude reflect sample inhomogeneities. Finally, we demonstrate the potential of FCS as a tool for quality control in production and optimization of biocompatible nanocrystals and present a comparative study of three promising modification chemistries.

MATERIALS AND METHODS

Samples. We investigated three different surface chemistries (four different particles, two having the same coating but different shell compositions) of water-stable CdSe/ZnS NCs that were synthesized and modified in our laboratory or purchased from Quantum Dot Corp. (Hayward, CA). NCs were chosen to emit at approximately the same wavelength, ~610 nm. CdSe core particles were coated with a higher band gap shell of ZnS (or CdS/ZnS) to increase quantum yield and photostability according to protocols described elsewhere.[7,14] NCs with the following surface chemistries were studied: (1) Peptide-coated NCs, CdSe/ZnS (pcNCs) and CdSe/CdS/ZnS (pcNCs(+Cd)) NCs were covered with phytochelatin-related peptides. The peptides have two distinct domains, a hydrophobic domain that is responsible for NC surface recognition and a hydrophilic domain that affords solubilization in aqueous buffer.[7] (2) Lipid-coated NCs (lcNCs), CdSe/ZnS NCs were encapsulated in phospholipid micelles following the protocol of Dubertret et al.[6] (3) QDots, NCs purchased from Quantum Dot Corp. consist of CdSe/ZnS core/shell and a proprietary amphiphilic polymer coat. The coat protects the NCs from environmental influences and provides stability in water. These NCs are further modified by conjugation to streptavidin as discussed in Wu et al.[5] (QDot 605 streptavidin conjugate, 1000-1).

(10) Kuno, M.; Fromm, D. P.; Hamann, H. F.; Gallagher, A.; Nesbitt, D. J. *J. Chem. Phys.* **2000**, *112*, 3117−3120.
(11) Shimizu, K. T.; Neuhauser, R. G.; Leatherdale, C. A.; Empedocles, S. A.; Woo, W. K.; Bawendi, M. G. *Phys. Rev. B* **2001**, *6320*, 5316, U5395−U5398.
(12) Ebenstein, Y.; Mokari, T.; Banin, U. *Appl, Phys, Lett.* **2002**, *80*, 4033.
(13) Hess, B. C.; Okhrimenko, I. G.; Davis, R. C.; Stevens, B. C.; Schulzke, Q. A.; Wright, Q. A.; Bass, C. D.; Evans, C. D.; Summers, S. L. *Phys, Rev, Lett.* **2001**, *86*, 3132−3135.
(14) Tsay, J. M.; Doose, S.; Pinaud, F.; Weiss, S. *J. Phys. Chem. B* **2005**, *109*, 1669−1674.
(15) Cordero, S. R.; Carson, P. J.; Estabrook, R. A.; Strouse, G. F.; Buratto, S. K. *J. Phys. Chem. B* **2000**, *104*, 12137−12142.
(16) Schlegel, G.; Bohnenberger, J.; Potapova, I.; Mews, A. *Phys. Rev. Lett.* **2002**, *88*, 137401.
(17) Fisher, B. R.; Eisler, H.-J.; Stott, N. E.; Bawendi, M. G. *J. Phys. Chem. B* **2004**, *108*, 143−148.
(18) Magde, D.; Elson, E. L.; Webb, W. W. *Biopolymers* **1974**, *13*, 29−61.
(19) Rigler, R.; Mets, U.; Widengren, J.; Kask, P. *Eur. Biophys. J.* **1993**, *22*, 169−175.
(20) Rigler, R.; Elson, E. S. *Fluorescence Correlation Spectroscopy: Theory and Applications*, 1st ed.; Springer-Verlag: Berlin, 2001.
(21) Hess, S. T.; Huang, S.; Heikal, A. A.; Webb, W. W. *Biochemistry* **2002**, *41*, 697−705.
(22) Krichevsky, O.; Bonnet, G. *Rep. Prog. Phys.* **2002**, *65*, 251−297.
(23) Bacia, K.; Schwille, P. *Methods* **2003**, *29*, 74−85.
(24) Larson, D. R.; Zipfel, W. R.; Williams, R. M.; Clark, S. W.; Bruchez, M. P.; Wise, F. W.; Webb, W. W. *Science* **2003**, *300*, 1434−1436.
(25) Enderlein, J.; Gregor, I.; Patra, D.; Fitter, J. *Curr. Pharm. Biotechnol.* **2004**, *5*, 155−161.
(26) Chiu, D. T.; Zare, R. N. *J. Am. Chem. Soc.* **1996**, *118*, 6512−6513.
(27) Chirico, G.; Fumagalli, C.; Baldini, G. *J. Phys. Chem. B* **2002**, *106*, 2508−2519.
(28) Osborne, M. A.; Balasubramanian, S.; Furey, W. S.; Klenerman, D. *J. Phys. Chem. B* **1998**, *102*, 3160−3167.

pcNCs and lcNCs were observed in distilled water (Millipore) whereas QDots were delivered and investigated in QDot buffer (Quantum Dot Corp.). For a comparison and as a control, 26-nm polystyrene beads (FluoSpheres, Molecular Probes Inc., Eugene, OR) with an absorption (emission) maximum at 535 nm (575 nm) and rhodamine 6G (R6G, Molecular Probes Inc.) were monitored in distilled water. The beads were briefly sonicated to exclude aggregation.

Optical Setup. All NC samples were characterized by absorption and emission measurements using a Lambda 25 UV/visible spectrometer (Perkin-Elmer Inc., Wellesley, MA) and a L-201M spectrofluorometer (PTI Inc., Lawrenceville, NJ). FCS measurements were performed using a custom-made confocal microscope based on a commercial inverted microscope (Axiovert 100, Zeiss, Germany). Laser excitation was performed by a Nd:YAG laser at 532 nm (Crysta Laser, Reno, NV) with powers in the range of 1−1000 μW as measured at the back focal plane of the water-immersion objective (1.2NA, 63x, Zeiss). The resulting excitation volume is on the order of 1 fl. Fluorescence was collected by the same objective and separated from excitation light by a dichroic mirror. A 50-μm pinhole was used to reject out-of-focus light. The signal was evenly split by a beam splitter cube and detected by two avalanche photodiodes (APDs, AQR-14, Perkin-Elmer Inc.). Detected photon pulses were sent to a hardware correlator card (ALV-6010, ALV GmbH, Langen, Germany), which computed the cross-correlation of the two channels with a temporal resolution of 6.5 ns. This configuration is insensitive to both APD dead times and afterpulsing. Simultaneous FCS measurements at two independent excitation powers were carried out by ALEX (details in Kapanidis et al.[29]) using an electrooptical modulator and polarization optics. Photon arrival times were recorded via a counter/timer computer board (PCI-6602, National Instruments) with a temporal resolution of 12.5 ns. Correlation of the two photon fluxes were correlated postrecording using custom-made software (developed in LabView, National Instruments). All FCS data were analyzed with the standard expression for two-dimensional diffusion in a Gaussian excitation volume:[19]

$$g(\tau) = [N(1 + \tau/\tau_D)]^{-1} \quad (1)$$

RESULTS AND DISCUSSION

Characterization of Photophysical Properties by FCS. Fluorescence correlation spectroscopy is sensitive to signal fluctuations caused by diffusion of individual molecules through the observation profile and fluctuations due to photophysics that result in additional signal intermittencies. We investigated the above specified NCs using FCS as a function of laser excitation power. Strong variations in the amplitude at zero correlation time $g^2(0)$ and in the overall shape of the correlation curve were observed as the excitation power was increased. These variations were significantly different from those observed for R6G in an identical experiment.

1. Overall Correlation Curve Shape Variations. FCS curves recorded on NCs exhibit a shape that can depart significantly from eq 1 depending on the excitation power and the NC modification. Typical behavior for QDots is shown in Figure 1 for excitation

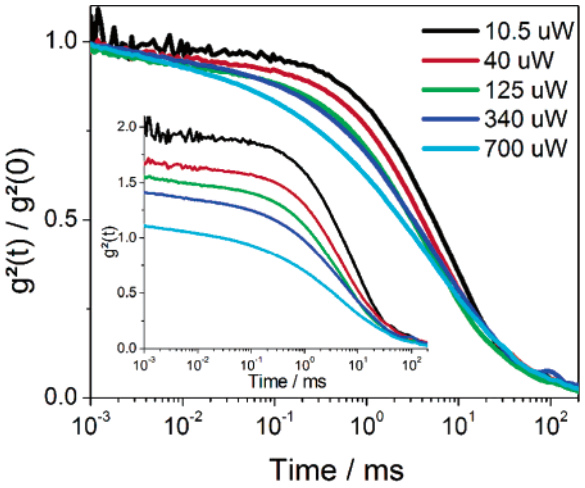

Figure 1. Typical FCS curves for NCs recorded at various excitation powers. Correlation functions $g^2(t)$ of QDots (inset) are normalized to $g^2(0)$ (main graph). Two distinct effects are visible with increasing excitation power: (1) the shape of the FCS curve deviates increasingly from a simple diffusion model (eq 1) due to photoinduced blinking; (2) $g^2(0)$ decreases (the apparent number of molecules $N = 1/g(0)$ increases) with increasing power.

powers varying from 1 to 1000 μW. The corresponding data for the other NC samples and R6G are given in the Supporting Information (Figure S-1). Organic dyes are known to exhibit blinking due to the population of long-lived triplet states, resulting in blinking on typically microsecond time scales. When FCS is performed on organic dyes with a high rate of intersystem crossing, a shoulder at microsecond-correlation times thus appears as the laser intensity is increased.[30] Blinking statistics of individual NCs have also been reported to change with excitation power, pointing to a photoinduced mechanism.[11] Therefore, changes in FCS curves as a function of excitation power could reflect changes in blinking parameters, as a result of this photoinduced mechanism.

In contrast to dyes, correlation curves of NCs lack a tripletlike shoulder (Figure 1). In fact, in some cases the flatness of certain correlation curves could incorrectly suggest very little or no blinking (Figure 2) since it could be fitted well to a simple FCS model that takes only diffusion into account (eq 1).[24] However, nonblinking NCs have never been observed in single-molecule assays under the given buffer conditions. In contrast to triplet blinking in organic dyes, NC blinking was determined to follow a power law statistics.[10] Since power law statistics do not exhibit a characteristic time scale (in contrast to exponential triplet kinetics), offperiods in NCs can be observed on any time scale with nonnegligible probability and thus influence FCS measurements on all time scales. An analytical expression of the correlation function combining diffusion and power law blinking (and thus overlapping time scales) has not yet been derived.

Since no analytical model exists to fit experimental NC-FCS data, we performed Monte Carlo simulations that include diffusion and power law on/off statistics to unravel the effects of NC blinking on FCS (details in Supporting Information). These simulations captured well the unusual shape of the correlation function (Figure 2). Simulations also showed that blinking

(29) Kapanidis, A. N.; Lee, N. K.; Laurence, T. A.; Doose, S.; Margeat, E.; Weiss, S. *Proc. Natl. Acad. Sci. U.S.A.* **2004**, *101*, 8936−8941.

(30) Widengren, J.; Mets, U.; Rigler, R. *J. Phys. Chem.* **1995**, *99*, 13368−13379.

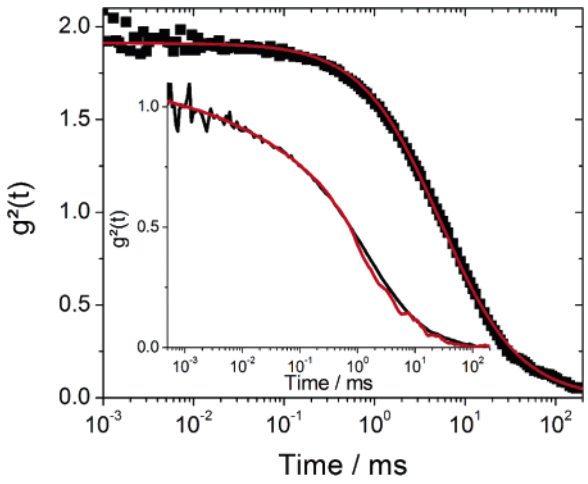

Figure 2. FCS data recorded from QDots at an excitation power of 10.5 μW (black) and fit (red) to a 2D diffusion model (eq 1). Inset: overlay of simulated (red) and measured (black) FCS data for NCs illustrating the influence of power law blinking on FCS curves. Experimental data are recorded from pcNCs at an excitation power of 450 μW. Simulations include power law blinking and diffusion through a Gaussian observation volume (Supporting Information).

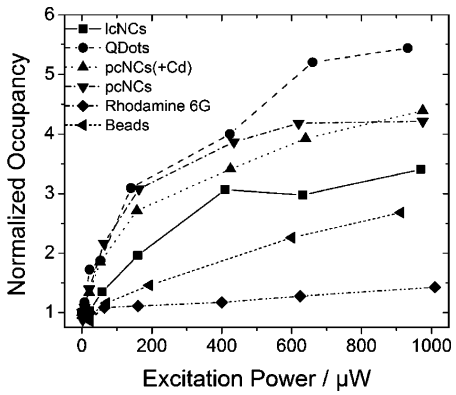

Figure 3. Occupancy N as a function of excitation power normalized to N(1 μW). Larger occupancies (lower FCS amplitudes as $N = \{1\}/\{g(0)\}$) are observed with increasing excitation power for all investigated samples. Whereas the increase for R6G and beads can be attributed to saturation effects, NC samples exhibit larger changes in N that do not correlate with saturation intensities (Table 1, Figure 7). The increase is attributed to blinking as photoinduced activation and optical trapping have been ruled out (Figure 3).

parameters exist for which FCS curves cannot be distinguished from a simple diffusion curve. The mere observation of a flat correlation curve that could be well fitted by a simple diffusion model does not prove the existence of nonblinking NCs and therefore could be erroneously interpreted.

Although providing qualitative agreement with experiments, these simulations cannot provide a numerical model for fitting blinking parameters. Power law statistics are only well defined if a lower cutoff time is introduced. Taking into account a power law distribution of both on- and off-times, four parameters are needed to fully describe the distribution: lower cutoff times and exponents for both on- and off-times. No one set of parameters could be uniquely mapped on simulated FCS curves. For this reason, it is currently not possible to extract power law parameters by comparing simulations with experimental data. A physical model that could provide a definition for the lower cutoff time is needed in order to make progress on this front.

2. Amplitude Changes. Another argument supporting the presence of blinking in all NCs investigated in this work relies on the observation that the amplitude at zero correlation time $g^2(0)$ changes more with increasing excitation power than can be explained by known factors (Figure 3). $g^2(0)$ is determined mostly by the concentration, or occupancy, of fluorescent molecules in the observation volume (occupancy $N = 1/g(0)$). Additional contributions come from (1) signal-to-background ratio (S/B)[19] and (2) effective broadening of the excitation profile due to signal saturation.[24,25]

In addition to (1) and (2), optical trapping, caused by radiation pressure,[31] may also influence $g^2(0)$. Several reports indeed suggested that optical trapping alters the apparent diffusion constant (and hence the residence time and local concentration) of molecules traversing the confocal volume.[26−28] To quantify possible optical trapping effects we performed FCS using an alternating-laser-excitation scheme (ALEX-FCS).[29] The laser excitation intensity was alternated between a low-level intensity (Int_1) and a high-level intensity (Int_2) with an alternation period of 50 μs (~10 times faster than the diffusion time—see Figure 4a). Since the alternation period is much faster than the residence time of the NCs or dyes in the confocal volume, optical trapping effects, if occurring, would be observed as increasing residence time and occupancy throughout alternation of excitation intensities. A series of measurements was taken with constant Int_1 but increasing Int_2. Photons that were emitted during the excitation with Int_1 and those that were emitted during the excitation with Int_2 were separately correlated. Occupancies N and diffusion times τ_D were extracted from the FCS curves by averaging out the periodic contribution to the correlation function that comes from the alternating laser excitation. If optical trapping effects were present, particles would be slowed during excitation period with Int_2, but the increase in residence time would be observed during the excitation with Int_1. If, however, only saturation or photophysics alter $N = 1/g(0)$ and τ_D, no "memory" in the diffusion would be observed. As can be seen in Figure 4b, N of pcNCs increases with increasing Int_2 while it is unchanged for the constant Int_1. Similar results were observed for R6G. The overall increase of N with increasing Int_2 is consistent with FCS measurements under constant laser excitation (Figure 3). Figure 4c shows the extracted diffusion times for Int_1 and Int_2, again excluding "memory" in the diffusion. The observed decrease in the diffusion time of R6G is due to photobleaching. If a fluorophore is photobleached within its translational diffusion time, the apparent diffusion time is reduced, whereas the fluorophore's contribution to the correlation amplitude is unchanged. The reduction in diffusion time is equally sensed for Int_1 and Int_2 as seen in Figure 4c.

These results indicate that the real local concentration does not change during the 25 μs of higher excitation (Int_2) intensity. We therefore conclude that optical forces do not increase the local concentration of either R6G or CdSe/ZnS pcNCs (Figure 4b) or polystyrene beads (data not shown). The results of Figure 4b,c also show that neither photoinduced activation nor photobleaching occur for the investigated NCs in the power range between 100 and 1000 μW. Significant influences from varying signal-to-

(31) Ashkin, A.; Dziedzic, J. M.; Bjorkholm, J. E.; Chu, S. *Opt. Lett.* **1986**, *11*, 288−229.

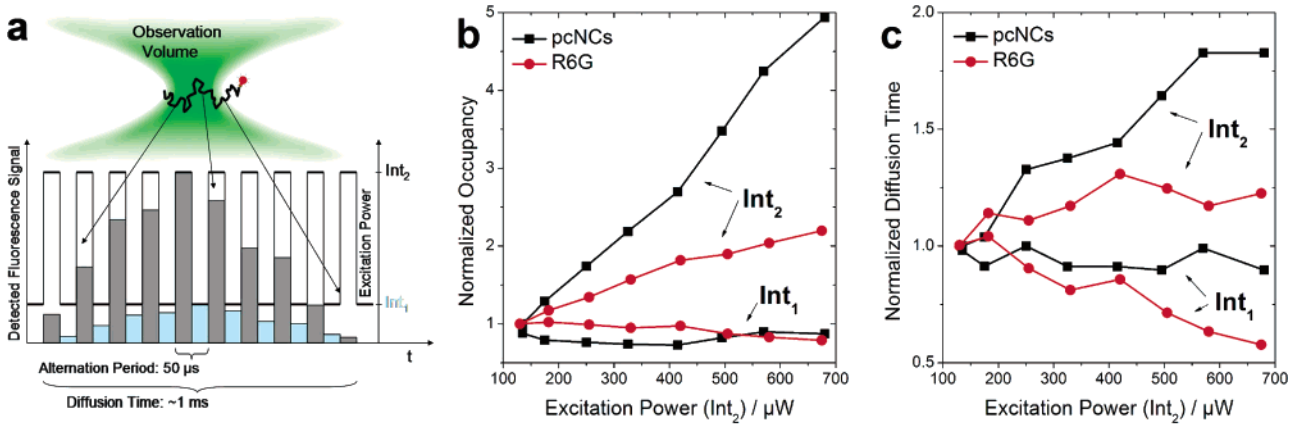

Figure 4. ALEX-FCS acquired for pcNCs (in water) and R6G (in water/50% glycerol). (a) FCS curves were calculated separately from photons emitted after excitation with Int_1 (blue) and those emitted after excitation with Int_2 (gray). The excitation intensity was alternated between Int_1 and Int_2 at a rate of 1/(50 μs) during each traversal of a molecule through the observation volume (green). Occupancy and diffusion time were extracted from both FCS curves and plotted as a function of Int_2. Each pair of data points, measured at given excitation intensities Int_1/Int_2, reflects an FCS measurement with a collection time of 300 s. (b) Occupancy under Int_2 for both pcNCs (black) and R6G (red) increases with Int_2 to the same degree as was observed in non-ALEX FCS (Figure 3). Occupancy under Int_1 remains constant, proving that the physical concentration in the observation volume is not changed under excitation with Int_2. (c) Diffusion times show equal behavior for pcNCs. In the case of R6G, photobleaching shortens the transient time of individual molecules. Once a molecule is photobleached, it is not visible in all remaining cycles under Int_1 as well as under Int_2, which causes diffusion times to decrease equally under Int_1 and Int_2.

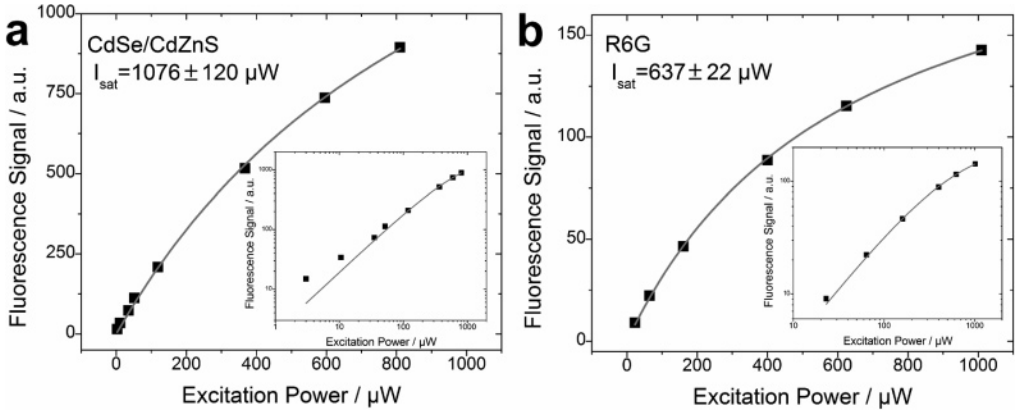

Figure 5. Observed average count rate (fluorescence signal) as a function of excitation power. The fluorescence signal $F(I)$ recorded for (a) pcNCs and (b) rhodamine 6G on a confocal microscope is saturated with increasing excitation power I. Saturation intensities I_S are extracted by fitting the data to a saturation function $F(I) = F(0)I/(I + I_S)$. Inset: The fluorescence signal of all investigated NCs deviates from the saturation function at very low excitation powers, as shown in a log−log representation. Saturation intensities for all samples are listed in Table 1.

background ratios (S/B) can also be excluded, as S/B > 20 (typically >100) results in a correction factor $F_{corr} = S^2/(S + B)^2 > 0.91$ (> 0.98).[19]

The remaining factors contributing to the intensity dependence of $g^2(0)$ must be saturation and blinking. Saturation could be caused either by changes in the fluorescence lifetime or by blinking itself. An estimation of the saturation intensity (in units of μW, measured before the objective) could be obtained from the integrated count rate (total number of accumulated photons during a measurement) as a function of excitation power. Since the ALEX-FCS experiment proved that no changes in the local concentration of fluorescent NCs were observed under increasing excitation power (due to optical trapping, to photoinduced activation of dark particles, or to photobleaching), the total count rate reflects emission properties of a constant number (concentration) of NCs.

Saturation curves were derived by plotting the average observed count rate as a function of excitation power I (Figure 5). The data were fitted to the saturation formula:

$$S = S_0 \frac{I}{I + I_S} \tag{2}$$

with I_s the saturation intensity, defined for organic dyes by

$$I_s = \frac{(\sigma\tau)^{-1}}{1 + k_{ISC}/k_{ph}} \tag{3}$$

In this expression, σ is the absorption cross section of the dye, τ its fluorescence lifetime, k_{ISC} the rate of intersystem crossing, and k_{ph} the rate of phosphorescence (return to the ground state from the triplet state).

On a linear scale, these fits appear to be satisfactory. For NCs, however, the fits are quite good over 2 orders of intensity magnitude but do not fit the curves well at very low intensities (inset Figure 5). This is not surprising since the dependence of NC blinking statistics on excitation power is not known yet, but most likely deviates from the exponential kinetics of triplet

Table 1. Photophysical and Colloidal Properties of All Investigated NCs

	diameter (nm)	saturation intensity (mW)	BPP (au)	quantum yield (%)	N/OD (au)
pcNCs	12.3 ± 2.4	1.07 ± 0.51	0.22 ± 0.04	1−9	0.55 ± 0.06
pcNCs(+Cd)	13.0 ± 1.1	1.00 ± 0.11	0.43 ± 0.09	15−24	0.64 ± 0.06
lcNCs	18.5 ± 1.7	0.44 ± 0.09	0.17 ± 0.03	15	1.00 ± 0.10
QDots	30.3 ± 3.2	0.53 ± 0.10	1.00 ± 0.20	59	0.53 ± 0.05
Beads	26.0 ± 1.9	0.27 ± 0.04	na[a]	na	na
R6G	na	0.64 ± 0.02	na	na	na

[a] na, not available.

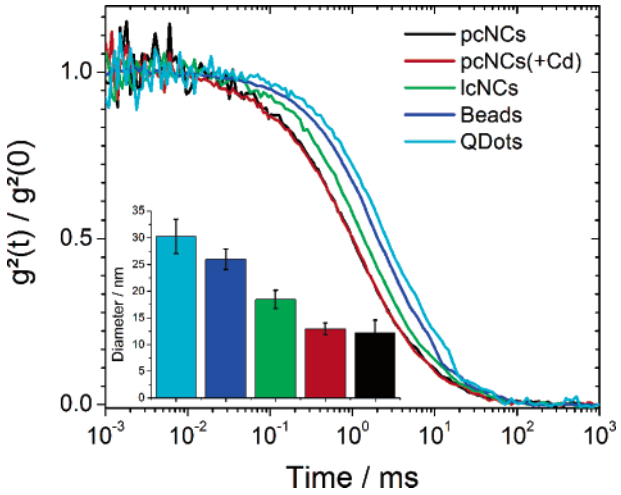

Figure 6. FCS data recorded for various NCs at low excitation power (~1 μW) and normalized to $g^2(0)$. Diffusion times were extracted by fitting the data to a simple diffusion model (eq 1). Particle diameters were calculated from diffusion times using the Stokes−Einstein equation and the bead size determined by TEM as calibration. Error bars represent standard deviations of repeated measurements.

blinking. We tabulated saturation intensities obtained from such fits for all studied NCs, beads, and R6G in Table 1. We found that the saturation intensity of lcNCs and QDots is on the same order of magnitude as R6G. Beads are found to saturate at half the excitation power whereas pcNCs have twice as large saturation intensity.

From Figure 3 it is clear that changes in the correlation amplitude $g^2(0)$ as function of laser intensity are considerably larger for all investigated NCs in comparison to R6G and beads. Assuming that the observed increase of N for R6G and beads is solely due to saturation, and comparing to NC results, we argue that saturation alone cannot account for the $g^2(0)$ changes of NCs. Since, in addition, we have shown that there are no changes in the NCs' local concentration in the observation volume due to photoinduced activation, photobleaching, or optical trapping, the only remaining explanation is changes in blinking statistics, induced by the laser light, that cause an apparent increase in the NC concentration.

As seen from Table 1 and Figure 7a, pcNCs have the highest saturation intensity. To provide evidence that the larger saturation intensity is also due to blinking behavior and not directly related to fluorescence lifetime, we measured the lifetime of lcNCs, QDots, and pcNCs. The fluorescence lifetimes were measured using TCSPC and are presented in the Supporting Information (Figure S-2). NCs are known to exhibit a nonexponential decay.[16,32] Figure S-2 shows shorter lifetimes for lcNCs and QDots as compared to pcNCs. Shorter lifetimes should in principle result in higher saturation intensities (eq 3), in contradiction with our observation. Since the measured lifetime differences do not correlate with differences in saturation intensity, the fluorescence lifetime cannot be the limiting mechanism for the saturation of NCs.

3. Relative Concentration Estimates. FCS measurements on NCs taken at very low excitation power often look like data from purely diffusing dyes (eq 1). As discussed above, this alone does not imply the absence of blinking. On the other hand, single-molecule studies of surface-immobilized NCs do indicate longer "on" periods (less blinking) at very low powers (Supporting Information Figure S-3). Under the assumption that blinking is negligible for extremely low excitation powers, we analyzed FCS curves to extract and compare occupancy and brightness per particle for pcNCs, lcNCs, and QDots.

The correlation amplitude is inversely proportional to the concentration of fluorescent particles, $c_{\text{bright}} = N/V_0 = 1/[V_0 V g^2(0)]$ (eq 1). We determined the relative number of molecules inside the observation volume V_0, the occupancy N, from FCS measurements at an excitation intensity of 1 μW. Such low excitation intensity (~1/100 of I_S) ensures measurement of the highest possible $g^2(0)$, minimizing the influence from blinking and excluding saturation effects. Assuming that light is mostly absorbed by inorganic core/shell material (with similar absorption cross sections for all NCs emitting at the same wavelength), the optical density provides an estimate of the total NC concentration c_{all} independent of their fluorescence:

$$\text{OD}_{350} = A\sigma c_{\text{all}} \tag{4}$$

where A is a numerical factor depending on the details of the ensemble measurement. From this it results that

$$N/\text{OD}_{350} = \frac{V_0}{A\sigma}\frac{c_{\text{bright}}}{c_{\text{all}}} \tag{5}$$

By comparing N with the optical density at 350 nm, OD_{350}, we find variations in the ratio N/OD_{350} for different NCs, which indicate the existence of a subpopulation of dark NCs that is not detected by FCS. Dark NCs were indeed observed by Ebenstein et al..[12] Variations in the observed occupancy could also be

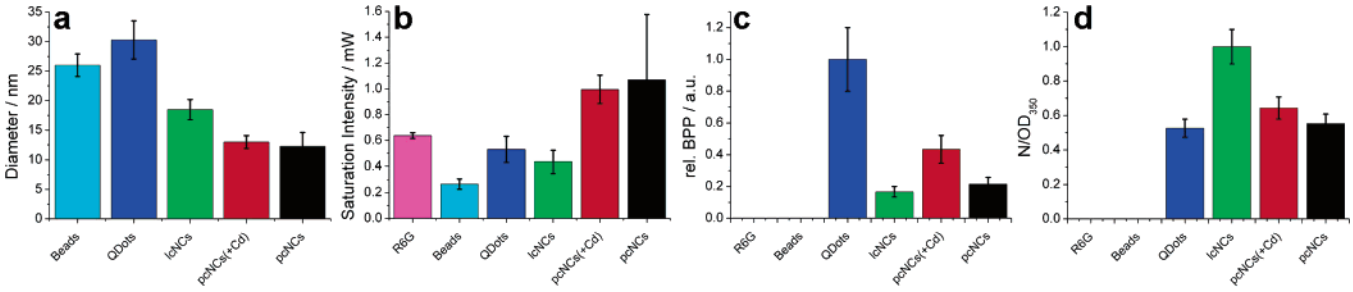

Figure 7. Colloidal and photophysical properties for all investigated NCs, beads, and R6G (according to Table 1). Particle size, BPP, and occupancy N were measured by FCS. Optical density OD_{350} was measured by ensemble absorption measurements. Saturation intensity was derived as presented in Figure 5. Error bars represent standard deviations of repeated measurements.

explained by the presence of small aggregates (aggregates of two or very few NCs would be detected in FCS as single NCs and thus decrease the ratio between occupancy and optical density). Table 1 and Figure 7d summarize $N/OD_{350}$of the various NCs. We found that N/OD_{350} of lcNCs is about twice as large as that of pcNCs and QDots. This result is consistent with Larsons's report that the ratio between measured (by 2P-FCS) and expected concentrations (from synthesis yields) is on the order of 0.5.[24] It further demonstrates that the fraction of NCs that is in a long-lived dark state or the amount of small aggregates depends on the applied surface chemistry. As photoinduced activation of dark NCs has been previously observed,[14] the ratio between bright and dark NCs seems to be dynamic and might therefore be shifted toward increasing the amount of bright NCs in three ways: light irradiation, optimization of inorganic coating,[14] and optimization of organic coating.

4. Brightness per Particle. The above result further points out that ensemble QYs do not necessarily describe the brightness of individual NCs. The brightness per particle (BPP) can be extracted by dividing the average detected signal by the occupancy N. This parameter is related to the bulk quantum yield, but would only be directly proportional to it if all particles were fluorescent ("bright"), which is generally not the case. Since BPP characterizes the fluorescence that can be observed from an individual NC, it is the more relevant parameter for single-molecule applications. We observed the highest BPP for QDots (Table 1 and Figure 7b). The BPP of lcNCs and CdSe/ZnS pcNCs was ~1/3 to ~1/5 of QDots BPP. The BPP of CdSe/CdS/ZnS pcNCs was ~1/2 of QDots BPP.

Since $QY = BPP N/OD_{350}\, A/V_0\, I_e$, where I_e is the excitation intensity, it is evident that a large QY can recover different cases of BPP and N/OD_{350} ratios. Depending on the exact application, optimization of NCs photophysical properties might require to increase BPP while retaining N/OD_{350} at its maximum value. Single-molecule applications for instance may favor NCs with a large BPP, but not necessarily large N/OD_{350}.

Characterization of Colloidal Properties by FCS. NCs have the potential to be used as single-molecule reporters in various applications. To fulfill this promise, adequate characterization not only of their photophysical but also of colloidal properties, precise stoichiometry, size distribution, and lack of aggregation in aqueous solution is needed.

1. Hydrodynamic Radius. The characteristic decay time in FCS reflects the diffusion constant of the observed molecule if saturation and photobleaching can be excluded. FCS can therefore be used to estimate the hydrodynamic radius assuming that NCs behave like spherical particles obeying the Stokes−Einstein equation $D = k_B T/6\pi\eta R$, where $k_B T$ is the thermal energy, η is the viscosity, and R is the particle radius.[33] We used polystyrene beads, characterized by TEM to have a diameter of 26 nm, as standard reference to estimate the NCs' hydrodynamic radii (listed in Table 1). The same FCS measurements as discussed above (excitation intensity ~1 μW) were analyzed with respect to diffusion times. Hydrodynamic diameters for CdSe/ZnS pcNCs were determined to be within 10−15 nm. This result is consistent with size exclusion gel chromatography (SE-HPLC) results.[7] Identical hydrodynamic diameters were measured for Cd-doped shells (pcNCs (+Cd)), confirming that doping does not change the particle's size.

The estimated diameter of the lcNCs was 18 ± 2 nm. Dubertret et al.[6] measured smaller values of 10−15 nm for lcNCs emitting at 550 nm by TEM. The discrepancy is most likely due to the size difference of the core NCs, which was observed to have a pronounced influence on the lipid coating.[6] Also diameters of dry samples measured by TEM are expected to be smaller than hydrodynamic diameters measured in solution. Diameters of 30 ± 3 nm were measured for QDots. This value agrees well with the size reported by Larson et al.[24]

2. Aggregation Properties. The correlation amplitude $g^2(0)$ is independent of the absolute signal for a homogeneous sample. However, if two populations with different brightness are present, $g^2(0)$ depends on the ratio of the concentration of the two populations and their relative brightness.[21] We recorded multiple FCS curves for a given sample with an integration time of 30 s each. This integration time is sufficiently long for extracting $g^2(0)$ with an acceptable signal-to-noise (S/N) ratio. A histogram of correlation amplitudes $g^2(0)$ extracted from 40 consecutive measurements for QDots and CdSe/CdS/ZnS pcNCs is shown in Figure 8. $g^2(0)$ scatter was present for all investigated NCs but was significantly larger for QDots compared to the other samples. A large $g^2(0)$ scatter in multiple successive measurements (on the same sample) indicates a large heterogeneity in brightness. Brightness heterogeneity could be the result of heterogeneity in quantum yields of individual NCs or the presence of small aggregates in the sample. The scatter was larger for aged samples, suggesting that aggregation was the most significant contributor.

(32) Dahan, M.; Laurence, T.; Pinaud, F.; Chemla, D. S.; Alivisatos, A. P.; Sauer, M.; Weiss, S. *Opt. Lett.* **2001**, *26*, 825−827.
(33) Einstein, A. *Ann, Phys,* **1905**, *17*, 549−560.

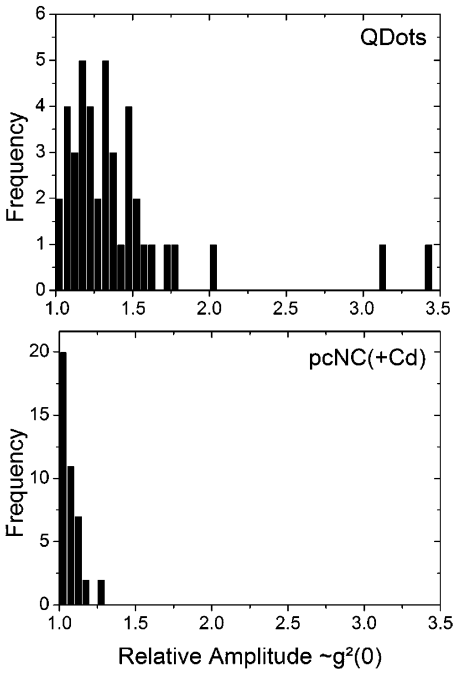

Figure 8. Histograms of $g^2(0)$ from multiple FCS measurements. FCS amplitudes were taken from 40 successive measurements on QDots and pcNCs(+Cd) (30 s integration time each, 26 μW excitation intensity), normalized to the smallest $g^2(0)$, and binned in intervals of 0.1. The data on QDots show a broader distribution than on pcNCs reflecting brightness inhomogeneities. These can be caused either by the presence of small aggregates or by a QY inhomogeneity in the sample.

CONCLUSION

In this work, we have utilized FCS for a comparative study of water-stable semiconductor NCs. We presented the potential of FCS to assess photophysical and colloidal properties that cannot be characterized by ensemble experiments. The advantage of single-molecule sensitivity becomes important as NCs have inhomogeneous properties with respect to brightness but are still promising fluorescent labels for single-molecule studies in cell biology. FCS measurements of NCs in solution at different intensities were shown to be a sensitive tool for unraveling blinking and saturation effects that are otherwise hidden in a single FCS curve. To establish relative concentrations of emitting particles, brightness per particle, saturation intensity, and particle size as quality parameters, we ruled out influences on FCS from saturation, power law blinking, and optical trapping, using results from ALEX-FCS and computer simulations. Such a set of parameters was acquired for pcNCs, pcNCs(+Cd), lcNCs, and QDots and shown to be consistent with independent ensemble measurements. Significant differences in hydrodynamic radius depending on the organic coating were found. In addition, our analysis could show significant differences in BPP, in the amount of dark particles for different NCs and in the propensity for aggregation which are not detectable by ensemble QY measurements. Whereas QDots have superior QYs as well as the largest BPP, pcNCs are shown to have desirable properties for single-molecule applications: they are smaller, have higher saturation intensities (possibly caused by less blinking), show no aggregation in aqueous solution, and can be used for single-molecule experiments in live cells.[7] We conclude that FCS constitutes a practical screening tool for the molecular evolution of unique organic−inorganic composite nanomaterials with unique, tailored properties.

ACKNOWLEDGMENT

We thank Xavier Michalet and Achillefs N. Kapanidis for helpful discussions and Xiangxu Kong and Thilo D. Lacoste for help with supporting data. We thank X.M. for critical reading of the manuscript. The research presented in this work is supported by NIH (grant 5-R01-EB000312), the Keck Foundation (grant 04074070), and DARPA/AFOSR (grant FA955004-10048). S.D. was supported by the Boehringer Ingelheim Fonds.

SUPPORTING INFORMATION AVAILABLE

FCS data for all investigated NCs; fluorescence lifetime data; confocal scans of surface-immobilized TOP/TOPO NCs at various excitation powers; description of Monte Carlo simulations. This material is available free of charge via the Internet at http://pubs.acs.org.

Received for review January 7, 2005. Accepted January 21, 2005.

AC050035N